Thermal Effects of Artificial Lamination Faults in a Three-Phase Transformer Core Using Infrared Thermography

Ehsan Altayef, Sofiane Chiheb, Fateh Anayi, Michael Packianather and Eheda Hassan

Abstract−Transformer core lamination faults can significantly affect transformer performance, reliability, and operational lifetime by increasing core losses and localized heating. This paper investigates the thermal effects of edge burr faults and inter-laminar insulation deterioration. An experimental test rig consisting of a 15 kVA three-phase transformer and a FLIR C2 thermal imaging camera was developed to capture temperature distributions under healthy and faulty operating conditions. Faults were introduced by creating controlled short circuits between laminations with varying affected areas and numbers of shorted laminations. Thermal images were acquired at different magnetic flux densities ranging from 0.5 T to 1.8 T under no-load conditions. The results demonstrate that both fault types produce noticeable temperature rises compared with healthy operation, with the severity of heating increasing as the flux density and fault size increase. Edge burr faults resulted in localized hot spots and temperature rises of up to 10% compared with healthy conditions, while insulation deterioration faults produced temperature increases exceeding 18% for severe fault scenarios at 1.8 T. The findings confirm that infrared thermography provides an effective non-invasive technique for detecting and assessing transformer core lamination faults and can support condition monitoring and early fault diagnosis in power transformers.

***Keywords*−Power transformer, Transformer core faults, Edge burrs, Lamination insulation degradation, Infrared thermography, Thermal imaging, Condition monitoring.**

I. INTRODUCTION

Power transformers are among the most critical and expensive assets in electrical power systems, serving as essential links between generation, transmission, and distribution networks. Their reliable operation is therefore vital for ensuring continuity of supply and maintaining the stability of modern power grids [1]–[6]. Although transformer failures can originate from several sources, defects associated with the magnetic core remain particularly important because they can develop gradually and remain undetected until significant damage has occurred [9], [18].

The transformer core is manufactured from thin grain-oriented electrical steel laminations insulated from one another to suppress eddy currents and minimize core losses [13]. The effectiveness of this design relies heavily on the integrity of the insulation coating between adjacent laminations. During manufacturing, transportation, installation, or long-term operation, the insulation layer may deteriorate or become damaged, leading to unintended electrical contact between laminations. Similarly, mechanical defects such as edge burrs can create localized short-circuit paths that increase circulating currents within the core [14], [15], [17]. These defects generate excessive heat, increase iron losses, accelerate insulation ageing, and may ultimately compromise transformer efficiency and reliability [18], [19].

Early detection of core lamination faults has attracted considerable attention in recent years. Various diagnostic techniques have been proposed, including no-load current analysis, vibration monitoring, acoustic emission methods, flux measurement, dissolved gas analysis, and frequency-response-based approaches [10]–[12], [25], [26]. While these techniques can provide valuable information regarding transformer condition, they often require complex signal processing, specialised equipment, or indirect interpretation of fault signatures. Furthermore, some methods may have limited sensitivity to localized defects in their early stages [11], [25].

Infrared thermography has emerged as a promising non-contact diagnostic tool for condition monitoring of electrical equipment [7], [8]. Since thermal abnormalities are frequently associated with increased losses and fault development, thermal imaging can provide direct visual evidence of abnormal operating conditions. In transformer cores, localized short circuits between laminations generate hot spots that can be detected through temperature distribution analysis [20]–[24]. Despite the growing interest in thermographic inspection, relatively few experimental studies have systematically investigated the thermal behaviour of different types of artificial lamination faults under controlled operating conditions and varying magnetic flux densities [21]–[24].

This paper presents an experimental investigation into the thermal effects of two common transformer core defects: edge burr faults and inter-laminar insulation deterioration. A dedicated fault-test platform based on a 15 kVA three-phase

Manuscript received June 28, 2026; accepted July 4, 2026.

Ehsan Altayef, Fateh Anayi, and M. Packianather are with School of Engineering Cardiff University, United Kingdom (e.altayef@gmail.com; Anayi@cardiff.ac.uk; . PackianatherMS@cardiff.ac.uk.)

Sofiance Chiheb is with National Higher School of Technology and Engineering, Annaba, Algeria (s.chiheb@ensti-annaba.dz)

Eheda Hassan is with University of Hertfordshire, United Kingdom (Eheda222@hotmail.com)

Digital Object Identifier (DOI): 10.53907/enpesj.v6i1.396

transformer was developed to simulate various fault severities by creating controlled short circuits between laminations. Thermal images were acquired using a FLIR infrared camera under healthy and faulty conditions for flux densities ranging from 0.5 T to 1.8 T. The objective is to quantify the relationship between fault severity, magnetic flux density, and temperature rise within the transformer core, thereby evaluating the effectiveness of thermal imaging as a diagnostic tool for detecting and assessing lamination-related faults.

The contributions of this work are threefold. First, a comprehensive experimental dataset of thermal responses for multiple artificial lamination fault scenarios is established. Second, the influence of fault size and flux density on transformer core temperature is analysed quantitatively. Third, the study demonstrates the capability of infrared thermography to distinguish between healthy and faulty operating conditions, providing valuable insight for future transformer condition monitoring and fault diagnosis systems. The experimental framework and fault scenarios investigated in this study build upon previous investigations of transformer core lamination faults and their effects on transformer performance [27]–[29]. Recent advances in transformer fault diagnosis and electrical machine analysis have also provided additional motivation for the present work [30]–[33].

II. Experimental Set-up and Sample

As complimentary studies for previous fault and estimation works (e.g., [30]-[33]), the paper treat transformer core faults. This section describes the data acquisition system and experimental procedure employed to investigate the effects of lamination faults in power transformers. The experimental fault-testing platform was developed by the Magnetics Group at the Cardiff School of Engineering to facilitate controlled fault simulation and thermal analysis. The system enables the identification of hotspot regions within the transformer core through thermal imaging. Figure 1 presents a photograph of the experimental setup together with a schematic representation of the measurement system..

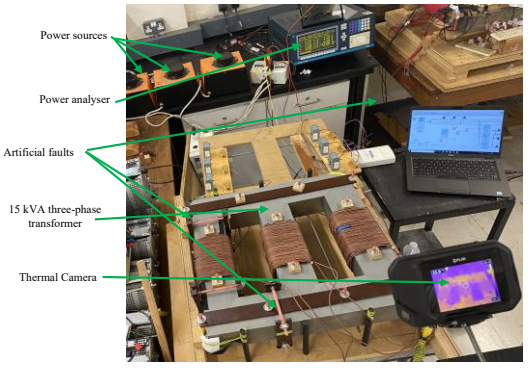

(a) Experimental setup

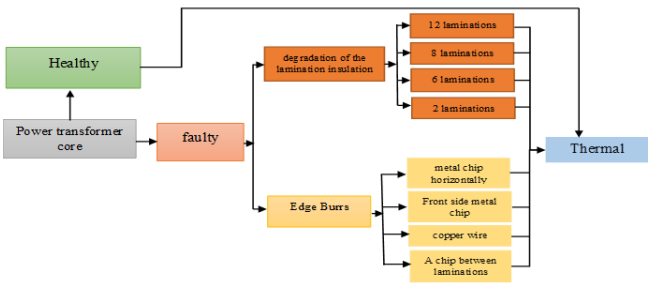

(b) Faulty operation diagram.

Fig. 1: Experimental Set-up

The experimental test rig comprises several key components, including a 15 kVA three-phase power transformer, specially designed clamping fixtures to secure the transformer during the introduction of edge burr faults, and a rotary tool used to remove approximately 400 mm² of insulation from the transformer core laminations to simulate the second fault condition investigated in this study. The magnetic flux density was determined from the measured voltage and current signals acquired using a power analyser connected to the transformer. A thermal imaging camera was employed throughout the experiments to capture the temperature distribution of both healthy and faulty transformer cores, enabling a comparative thermal analysis.

The transformer core is constructed from a stack of 520 grain-oriented electrical steel laminations. It features a dual-window core structure with window dimensions of 320 mm × 120 mm and overall core dimensions of 540 mm × 520 mm. Furthermore, both the primary and secondary windings are uniformly wound around the core limbs, each consisting of 50 turns of insulated copper conductor with a cross-sectional area of 1.5 mm².

III. Proposed Faults Details

A. Artificial Lamination Faults

In this study, two common transformer core faults were investigated: edge burrs and interlaminar insulation deterioration. These faults are among the most frequently occurring defects in transformer cores and can significantly affect transformer performance. To evaluate their impact, no-load tests were conducted, as no-load current measurements provide an indication of the transformer's no-load (iron) losses. During these tests, the transformer primary winding was energised with its rated voltage of 220 V, while the secondary winding remained open-circuited.

To assess the thermal effects of the investigated faults, the transformer was first examined under healthy operating conditions to establish a baseline for comparison. During this stage, the three-phase voltage and current were recorded at magnetic flux densities of 0.5, 0.8, 1.0, 1.5, 1.7, and 1.8 T. Each experiment was repeated three times to ensure the accuracy, repeatability, and reliability of the measured data. Furthermore, the data for each fault condition were collected on separate days, allowing sufficient time for the transformer core to return to ambient temperature before subsequent measurements. This procedure minimised the influence of residual heating on the experimental results. The following sections describe each fault condition in detail.

B. Edge Burr Fault

To simulate the edge burr fault, an artificial short circuit was introduced between adjacent laminations of the transformer core. Four fault scenarios were considered, each representing a different number of short-circuited laminations (i.e., different affected areas). Prior to fault implementation, baseline measurements were obtained under healthy operating conditions over a range of magnetic flux densities from 0.5 T to 1.8 T to establish a reference for comparison.

Following the baseline measurements, edge burr faults were introduced at various locations on the transformer core according to the predefined fault scenarios. A custom-designed clamping device, shown in Figure 2, was developed to fit the experimental transformer core used in this study. The clamping mechanism ensured firm and consistent electrical contact

between the artificial burr material and the edges of the laminated core stack, thereby providing repeatable and reliable fault conditions throughout the experiments.

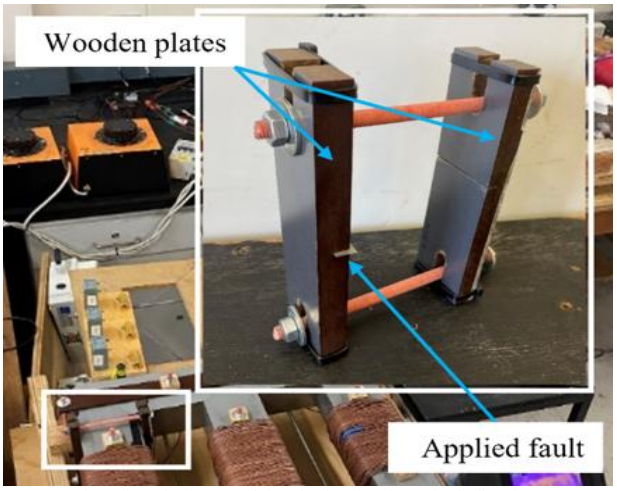

Fig. 2: Clamping device used for the laminations fault fixation

As illustrated in Figure 2, the clamping device consists of two wooden plates fastened using two plastic bolts, which apply uniform pressure to the copper foil placed on both sides of the laminated core stack. Since both wood and plastic are non-conductive and exhibit negligible electromagnetic interference, their influence on the experimental measurements can be considered insignificant. This assumption is consistent with previous studies, which have similarly neglected the effect of the clamping device on the experimental results (e.g., [19], [27]).

Four edge burr fault scenarios were implemented by varying the number of short-circuited laminations and the corresponding contact area, as illustrated in Figure 3. In the first scenario (Figure 3(a)), a thin metal strip was inserted to create a short circuit between two adjacent laminations within the 520-lamination transformer core. The contact area measured 45 mm in length and 0.5 mm in width, corresponding to an affected area of 22.5 mm².

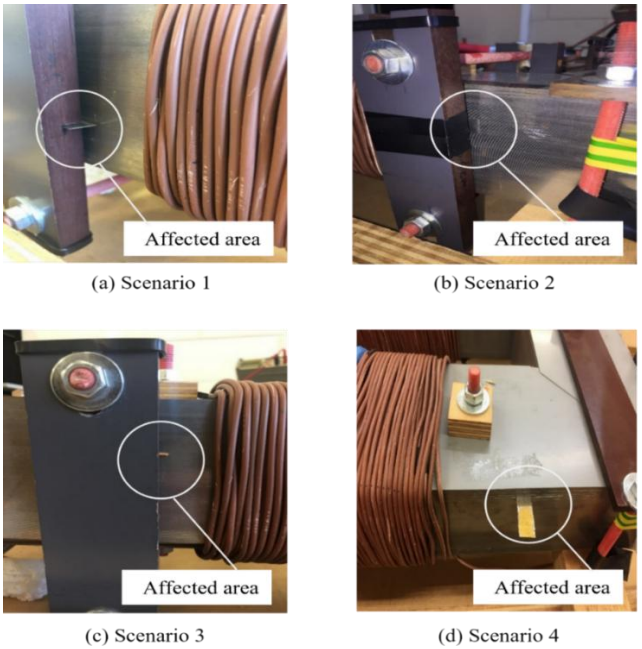

(a) Scenario 1 (b) Scenario 2

(c) Scenario 3 (d) Scenario 4

Fig. 3: Artificial edge burr lamination faults (a) scenario 1, (b) scenario 2, (c) scenario 3 and (d) scenario 4

the second scenario (Figure 3(b)), a wider metal strip measuring 45 mm × 10 mm was employed, producing a contact area of 450 mm². This configuration increased the number of short-circuited laminations from two to approximately 33, thereby representing a more severe edge burr fault.

For the third scenario (Figure 3(c)), a copper wire with a diameter of 1.3 mm was used to establish a short circuit across four adjacent laminations. The resulting contact area measured approximately 45 mm × 1.3 mm (58.5 mm²).

The fourth fault scenario, shown in Figure 3(d), consisted of a localized short circuit between two laminations with a contact area of 9 mm × 15 mm (135 mm²). This configuration was included to investigate the influence of contact geometry on the thermal behaviour of the transformer core.

C. Lamination Insulation Fault

Transformer cores are constructed from thin electrical steel laminations to minimise eddy current losses and improve operating efficiency. Each lamination is coated on both sides with a thin inorganic insulating layer, typically 1–3 µm thick, to prevent direct electrical contact between adjacent laminations. However, deterioration of the inter-laminar insulation may occur due to several factors, including ageing of the insulating coating, mechanical damage caused by external objects, and overheating resulting from winding failures or other abnormal operating conditions [29].

To investigate the thermal effects of inter-laminar insulation deterioration, artificial insulation faults were introduced into the transformer core, and thermal images were captured to assess the resulting temperature distribution. The fault was created by carefully removing the insulating coating from the selected laminations and inserting a copper strip between them to maintain electrical contact, thereby simulating insulation breakdown. The fault preparation procedure is illustrated in Figure 4.

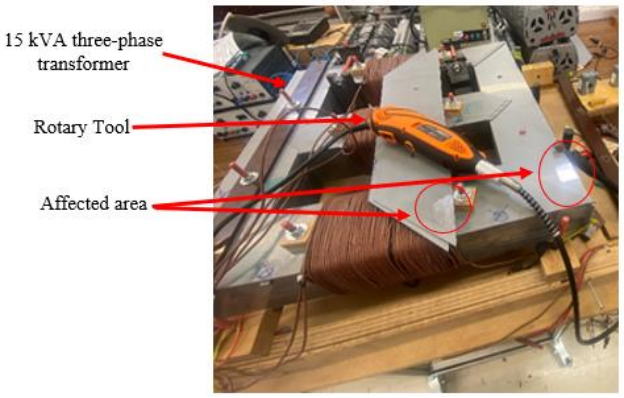

Fig. 4: Experimental setup used for the laminations fault analysis

To simulate inter-laminar insulation deterioration, artificial insulation damage was introduced on the opposing surfaces of selected transformer core laminations. Fault conditions involving short circuits between 2, 6, 8, and 12 laminations were investigated at magnetic flux densities of 0.5, 1.0, 1.5, 1.7, and 1.8 T. The insulation damage was created by removing approximately 40 mm² of the insulating coating using a rotary tool, thereby establishing electrical contact between adjacent laminations. To evaluate the influence of fault location on the transformer's thermal behaviour, the artificial faults were introduced at different positions within the transformer core.

IV. Healthy Operation Mode

This section presents the experimental results obtained from the thermal analysis of the transformer under healthy and faulty operating conditions. Thermal images were captured at various

magnetic flux density levels to evaluate the influence of the investigated lamination faults on the transformer core temperature distribution. A FLIR C2 thermal imaging camera was used to record all thermal images. For each fault scenario and flux density level, six thermal images with a resolution of 80 × 60 pixels were captured at 15-minute intervals throughout the experimental period. This acquisition procedure ensured consistent monitoring of the temperature evolution under each operating condition. The specifications of the FLIR C2 thermal camera are summarised in Table 1.

Fig. 5: Thermal camera

The specifications of the camera are presented in table 1.

TABLE 1 SPECIFICATIONS OF THE CAMERA

	PARAMETER	VALUE
1	Focal length	1.54 mm
2	Size (L*W*H)	124.46*78.74*12.44 mm
3	IR sensor	80*60 (4,800 measurement pixel)
4	Operating temperature range	-10°C to +50°C
5	Storage temperature range	-40°C to +70°C
6	Digital camera	640*480 pixel
7	Image frequency	9 Hz
8	Accuracy	±2°C
9	Thermal sensitivity	< 0.10°C

The thermal analysis was performed by first capturing thermal images of the transformer core under healthy operating conditions to establish a reference for comparison with the faulty conditions. These reference images provided a baseline for evaluating the temperature variations caused by the introduced lamination faults.

Although the FLIR C2 thermal camera has a relatively low image resolution compared with more recent thermal imaging systems, it was sufficient to identify the temperature distribution and hotspot locations associated with the investigated faults. Since the induced faults were located at the edges of the transformer core laminations, thermal images were captured from the side profiles of the transformer rather than the front surface. This viewing angle provided a clearer representation of the fault-affected regions and enabled more accurate observation of the corresponding thermal patterns, as illustrated in Figure 6.

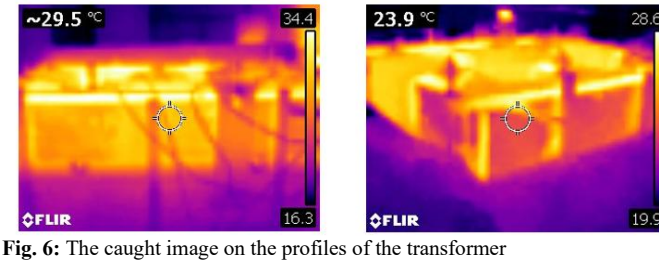

Fig. 6: The caught image on the profiles of the transformer

For improved visualisation, Figure 7 presents the thermal images of the transformer core under healthy operating conditions prior to the introduction of any faults. These images serve as a reference for evaluating the thermal effects of the investigated lamination faults. The maximum and minimum temperatures obtained from each thermal image provide a clear representation of the transformer core temperature distribution at different magnetic flux density levels. These temperature values were subsequently extracted as input features for the fault detection and classification process described in the following section.

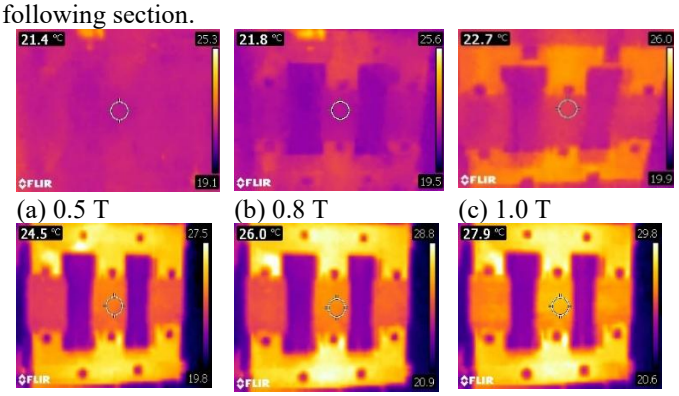

(a) 0.5 T (b) 0.8 T (c) 1.0 T

(d) 1.5 T (e) 1.7 T (f) 1.8 T

Fig. 7: Healthy operation mode results

For the healthy operating condition of the transformer core, it is observed that magnetic flux density has a significant influence on the temperature rise in the no-load transformer. At low flux density levels, as shown in Figure 7(a), the core temperature remains relatively low, with maximum and minimum values of approximately 25.3 °C and 19.1 °C, respectively. In contrast, at the highest flux density of 1.8 T (Figure 7(f)), a noticeable increase in temperature is observed, with maximum and minimum values rising to approximately 29.8 °C and 23.3 °C, respectively. This trend clearly indicates that higher magnetic flux densities lead to increased core heating under no-load conditions.

V. Faulty Operation Mode

A. Edge Burrs fault

This section presents the thermal imaging results for the first type of fault considered in this study, namely the edge burr fault. This fault was implemented at different scenarios and locations within the transformer core to evaluate its thermal impact. Figures 8 and 9 illustrate representative thermal images obtained at magnetic flux densities of 0.5 T and 1.8 T for fault scenarios 1 and 4, respectively. These figures are provided to demonstrate the influence of magnetic flux density on the temperature distribution of the transformer core under edge burr fault conditions.

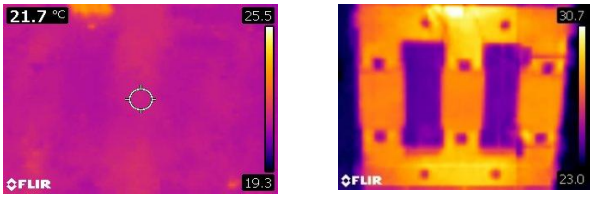

Fig. 8: Scenario 1 faulty operation mode results

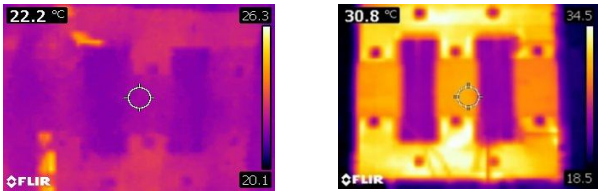

Fig. 9: Scenario 4 faulty operation mode results

The obtained thermal images indicate a clear difference between the temperature distribution under edge burr fault

conditions and that observed during healthy operation. This confirms that edge burr faults have a significant impact on the transformer core temperature and, consequently, on overall transformer performance. In general, an increase in temperature is observed across all fault scenarios.

For example, at a magnetic flux density of 1.8 T, the temperature under healthy conditions is approximately 1 °C lower than that observed in fault scenario 1. A more pronounced increase is observed in scenario 4, where the temperature is approximately 5 °C higher than the healthy condition. Furthermore, scenario 4 exhibits an increase of around 4 °C compared with scenario 1 at the same flux density. These results demonstrate that the rate of temperature rise becomes more significant with increasing magnetic flux density and a higher number of affected laminations within the transformer core.

Edge burr faults lead to increased core temperature, which in turn contributes to higher core losses and increased current losses. This temperature rise may also degrade the properties of the insulating materials, thereby reducing transformer efficiency and operational reliability. For this reason, further investigation of such faults in high-capacity transformers is strongly recommended.

Overall, the thermal imaging results show that edge burr faults can increase transformer core temperature by approximately 3.2% in scenario 1 compared with healthy conditions, and up to approximately 16.1% in scenario 4. In addition, scenario 4 exhibits a temperature increase of about 12.5% relative to scenario 1, indicating a clear relationship between fault severity and thermal response. These findings confirm that both magnetic flux density and the extent of lamination short-circuiting play a critical role in determining the thermal behaviour of the transformer core.

Lamination Insulation Faults

In this section, the thermal imaging results for the second type of fault, namely inter-laminar insulation degradation, are presented. This fault was introduced by selectively removing the insulating coating from the transformer core laminations, thereby creating electrical contact between adjacent layers. Figure 10 illustrates the corresponding thermal images of the transformer core under fault conditions.

The results correspond to short-circuit conditions involving 2, 6, 8, and 12 affected laminations, evaluated at magnetic flux densities of 0.5 T and 1.8 T. It should be noted that the influence of fault location on the position of the inter-laminar short circuit has been previously investigated using current signal analysis in [27]. In this study, the same fault placement strategy and positioning methodology were adopted to ensure consistency and comparability of results.

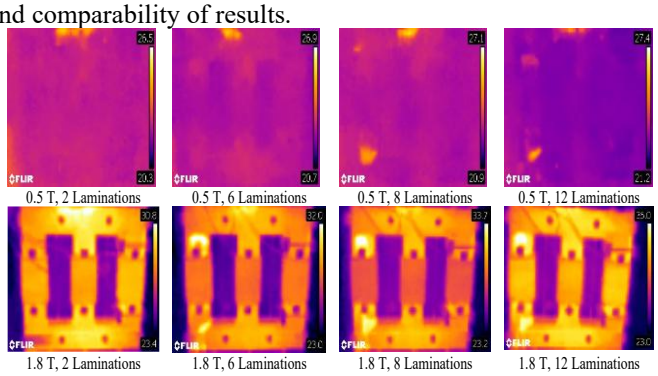

Fig. 10: Faulty operation mode results at 0.5 and 1.8 T

From the results presented in this figure, it is evident that the size of the fault, defined by the number of short-circuited laminations, has a significant influence on the transformer core temperature. The thermal measurements indicate that the temperature increases as the number of affected laminations increases, as illustrated in the figure. Specifically, the figure presents the maximum and minimum temperature values as a function of the number of affected laminations at magnetic flux densities of 0.5 T and 1.8 T.

The results demonstrate that the temperature rise associated with inter-laminar insulation faults is strongly dependent on both the number of shorted laminations and the applied flux density. For fault cases involving 2, 6, 8, and 12 short-circuited laminations, the highest temperatures are observed at a flux density of 1.8 T, with increases exceeding 9 °C compared with the corresponding values at 0.5 T for the 12-lamination fault scenario. For the case of two shorted laminations, the temperature increases by more than 4 °C across the flux density range from 0.5 T to 1.8 T. In addition, temperature rises of approximately 6 °C are observed for the six- and eight-lamination fault cases over the same flux density range.

Overall, the transformer core temperature under insulation degradation faults increases with both the severity of the fault (number of short-circuited laminations) and the magnetic flux density. This pronounced temperature rise may lead to increased core losses, particularly eddy current losses, which can reduce transformer efficiency and, in severe cases, contribute to operational failure.

Finally, the thermal data acquired using the FLIR C2 camera were stored in the device's internal memory and subsequently transferred to a personal computer for post-processing and feature extraction.

VI. Conclusion

This paper has presented an experimental investigation into the thermal behaviour of a three-phase transformer core under healthy and faulty lamination conditions using infrared thermography. Two common transformer core defects, namely edge burr faults and lamination insulation deterioration, were artificially introduced into a 15 kVA transformer core and analysed at different magnetic flux densities ranging from 0.5 T to 1.8 T.

The thermal imaging results demonstrated that both fault types cause significant temperature increases compared with healthy operating conditions. For edge burr faults, the transformer core temperature increased with both the flux density and the extent of the short-circuited lamination area. The largest edge burr scenario produced temperature rises of approximately 5 °C above healthy conditions at 1.8 T. Similarly, insulation deterioration faults generated progressively higher temperatures as the number of short-circuited laminations increased. The most severe insulation fault scenario, involving twelve affected laminations, produced temperature increases exceeding 9 °C at high flux density.

The experimental findings indicate that lamination faults create additional eddy-current paths, leading to increased core losses and localized hot spots that may accelerate insulation ageing and reduce transformer efficiency and reliability. Furthermore, the results confirm that thermal imaging is a practical, non-invasive, and effective diagnostic technique for identifying transformer core lamination defects and evaluating their severity.

Future work will focus on advanced thermal image processing and machine learning techniques for automatic fault detection, classification, and severity assessment, as well as extending the investigation to larger power transformers operating under practical loading conditions.

REFERENCES

[1] *P. Chen, Y. Huang, F. J. Zeng, Y. Jin, X. Zhao, and J. Wang, "Review on insulation and reliability of dry-type transformer," in Proc. IEEE Sustainable Power and Energy Conference (iSPEC), 2019, pp. 398–402.*

[2] *X. Duan, T. Zhao, J. Liu, L. Zhang, and L. Zou, "Analysis of winding vibration characteristics of power transformers based on the finite-element method," Energies, vol. 11, no. 9, 2018.*

[3] *C. Jettanasen and A. Ngaopitakkul, "A novel probabilistic neural network-based algorithm for classifying internal fault in transformer windings," IEEJ Transactions on Electrical and Electronic Engineering, vol. 8, no. 2, pp. 123–131, 2013.*

[4] *F. Yuan, J. Guo, Z. Xiao, B. Zeng, W. Zhu, and S. Huang, "A transformer fault diagnosis model based on chemical reaction optimization and twin support vector machine," Energies, vol. 12, no. 5, 2019.*

[5] *B. E. Lee, J. W. Park, P. A. Crossley, and Y. C. Kang, "Induced voltages ratio-based algorithm for fault detection, and faulted phase and winding identification of a three-winding power transformer," Energies, vol. 7, no. 9, pp. 6031–6049, 2014.*

[6] *M. Gutten, D. Korenciak, M. Kucera, R. Janura, A. Glowacz, and E. Kantoch, "Frequency and time fault diagnosis methods of power transformers," Measurement Science Review, vol. 18, no. 4, pp. 162–167, 2018.*

[7] *A. Sedighi, A. Kafiri, M. Shahnazari, M. R. Sehati, and F. Behdad, "Aging assessment of distribution transformers based on thermal imaging," in Proc. IEEE International Conference on Environment and Electrical Engineering and IEEE Industrial and Commercial Power Systems Europe (EEEIC/I&CPS Europe), 2019.*

[8] *A. S. N. Huda and S. Taib, "Application of infrared thermography for predictive/preventive maintenance of thermal defect in electrical equipment," Applied Thermal Engineering, vol. 61, no. 2, pp. 220–227, 2013.*

[9] *R. Murugan and R. Ramasamy, "Failure analysis of power transformer for effective maintenance planning in electric utilities," Engineering Failure Analysis, vol. 55, pp. 182–192, 2015.*

[10] *D. A. K. Pham, T. M. T. Pham, H. Borsi, and E. Gockenbach, "A new method for purposes of failure diagnostics and FRA interpretation applicable to power transformers," IEEE Transactions on Dielectrics and Electrical Insulation, vol. 20, no. 6, pp. 2026–2034, 2013.*

[11] *R. Khalili Senobari, J. Sadeh, and H. Borsi, "Frequency response analysis (FRA) of transformers as a tool for fault detection and location: A review," Electric Power Systems Research, vol. 155, pp. 172–183, 2018.*

[12] *M. Bagheri, A. Zollanvari, and S. Nezhivenko, "Transformer fault condition prognosis using vibration signals over cloud environment," IEEE Access, vol. 6, pp. 9862–9874, 2018.*

[13] *S. B. Lee, G. B. Kliman, M. R. Shah, W. T. Mall, N. K. Nair, and R. M. Lusted, "An advanced technique for detecting inter-laminar stator core faults in large electric machines," IEEE Transactions on Industry Applications, vol. 41, no. 5, pp. 1185–1193, 2005.*

[14] *A. Kedous-Lebouc, B. Cornut, J. C. Perrier, P. Manfé, and T. Chevalier, "Punching influence on magnetic properties of the stator teeth of an induction motor," Journal of Magnetism and Magnetic Materials, vols. 254–255, pp. 124–126, 2003.*

[15] *P. Handgruber, A. Stermecki, O. Biro, and G. Ofnery, "Evaluation of interlaminar eddy currents in induction machines," in Proc. IECON Annual Conference of the IEEE Industrial Electronics Society, 2013, pp. 2792–2797.*

[16] *M. Bigdeli, M. Vakilian, and E. Rahimpour, "Transformer winding faults classification based on transfer function analysis by support vector machine," IET Electric Power Applications, vol. 6, no. 5, pp. 268–276, 2012.*

[17] *M. B. Aimoniotis and A. J. Moses, "Evaluation of induced eddy currents in transformer sheets due to edge-burrs, employing computer aided design programs," in Proc. Athens Power Tech International Power Conference, vol. 2, pp. 847–850, 1993.*

[18] *E. Altayef, F. Anayi, and M. Packianather, "Power transformer fault detection methods and effects of edge burrs fault: A review," in Proc. 2nd International Conference on Advance Computing and Innovative Technologies in Engineering (ICACITE), 2022.*

[19] *R. Mazurek, H. Hamzehbahmani, A. J. Moses, P. I. Anderson, F. J. Anayi, and T. Belgrand, "Effect of artificial burrs on local power loss in a three-phase transformer core," IEEE Transactions on Magnetics, vol. 48, no. 4, pp. 1653–1656, 2012.*

[20] *V. M. Shiljkut, "Remote monitoring of power transformers thermal image," pp. 12–15, 2012.*

[21] *Y. Sun et al., "A temperature-based fault pre-warning method for the dry-type transformer in the offshore oil platform," International Journal of Electrical Power & Energy Systems, vol. 123, 2020.*

[22] *E. Gockenbach, P. Werle, and H. Borsi, "Monitoring and diagnostic systems for dry type transformers," in Proc. IEEE International Conference on Conduction and Breakdown in Solid Dielectrics, 2001, pp. 291–294.*

[23] *H. Li, "Thermal fault detection and diagnosis of electrical equipment based on the infrared image segmentation algorithm," Advances in Multimedia, vol. 2021, pp. 1–7, 2021.*

[24] *A. K. Al-Musawi, F. Anayi, and M. Packianather, "Three-phase induction motor fault detection based on thermal image segmentation," Infrared Physics & Technology, vol. 104, Art. no. 103140, 2020.*

[25] *M. Bagheri, M. Naderi, and T. Blackburn, "Advanced transformer winding deformation diagnosis: Moving from off-line to on-line," IEEE Transactions on Dielectrics and Electrical Insulation, vol. 19, no. 6, pp. 1860–1870, 2012.*

[26] *J. Liu, Z. Zhao, C. Tang, C. Yao, C. Li, and S. Islam, "Classifying transformer winding deformation fault types and degrees using FRA based on support vector machine," IEEE Access, vol. 7, pp. 112494–112504, 2019.*

[27] *E. Altayef, F. Anayi, M. S. Packianather, and O. Kherif, "On the effects of lamination artificial faults in a 15 kVA three-phase transformer core," IEEE Access, vol. 10, pp. 19348–19355, 2022.*

[28] *E. Altayef, F. Anayi, M. Packianather, Y. Benmahamed, and O. Kherif, "Detection and classification of lamination faults in a 15 kVA three-phase transformer core using SVM, KNN and DT algorithms," IEEE Access, vol. 10, pp. 50925–50932, 2022.*

[29] *E. Altayef, F. Anayi, and M. Packianather, "Experimental investigation on impacts of insulation damage fault between laminations of power transformers," in Proc. 2nd International Conference on Advance Computing and Innovative Technologies in Engineering (ICACITE), 2022.*

[30] *O. Kherif et al., "A New Multi-Path Hybrid Classifier for Transformer Oil Fault Diagnostic," ENP Engineering Science Journal, vol. 5, no. 2, Dec. 2025.*

[31] *A. Khelafi, A. Djebli, O. Touhami, and R. Ibtiouen, "Analysis of Multiphase Electrical Systems According to the Number of Phases," ENP Engineering Science Journal, vol. 4, no. 2, Dec. 2024.*

[32] *F. Leguebedj and D. Boukhetala, "Estimation of Synchronous Machine Parameters by Stand Still Frequency Responses Testing," ENP Engineering Science Journal, vol. 3, no. 2, Dec. 2023.*

[33] *O. Kherif, T. Zebbadji, Y. Gherbi, M. L. Azzouze, and M. Teguar, "Simplified Diagnosis Method for CHBMIs under Open-Circuit Switch or Battery Failure," ENP Engineering Science Journal, vol. 1, no. 2, Dec. 2021.*